Vector and tensor analyzing powers of elastic deuteron-proton scattering at 130 MeV deuteron beam energy

E. Stephan,[1,*] St. Kistryn,[2] R. Sworst,[2] A. Biegun,[1] K. Bodek,[2] I. Ciepał,[2] A. Deltuva,[3] E. Epelbaum,[4] A. Fonseca,[3] W. Glöckle,[5] J. Golak,[2] N. Kalantar-Nayestanaki,[6] H. Kamada,[7] M. Kiš,[6] A. Kozela,[8] M. Mahjour-Shafiei,[6,†] A. Micherdzińska,[1,‡] A. Nogga,[4] P. U. Sauer,[9] R. Skibiński,[2] H. Witała,[2] J. Zejma,[2] and W. Zipper[1]

[1]*Institute of Physics, University of Silesia, PL-40007 Katowice, Poland*
[2]*Institute of Physics, Jagiellonian University, PL-30059 Kraków, Poland*
[3]*Centro de Física Nuclear da Universidade de Lisboa, P-1649-003 Lisboa, Portugal*
[4]*Forschungszentrum Jülich, Institut für Kernphysik (Theorie), D-52425 Jülich, Germany*
[5]*Institut für Theoretische Physik II, Ruhr Universität Bochum, D-44780 Bochum, Germany*
[6]*Kernfysisch Versneller Instituut, University of Groningen, NL-9747 AA Groningen, The Netherlands*
[7]*Department of Physics, Kyushu Institute of Technology, Kitakyushu 804-8550, Japan*
[8]*Institute of Nuclear Physics, PL-31342 Kraków, Poland*
[9]*ITP, Universität Hannover, D-30167 Hannover, Germany*

(Received 17 June 2007; published 2 November 2007)

High precision vector and tensor analyzing power data of the deuteron-proton elastic scattering at 130 MeV deuteron beam energy have been measured in a large range of angles. They are compared with theoretical predictions obtained in various approaches: with realistic potentials for pure NN interactions, with the inclusion of a three-nucleon force, and in the framework of chiral perturbation theory. All the theoretical calculations describe roughly the main features of the measured distributions, but none of them can reproduce all their details. This indicates the need for further development of the three-nucleon force models.

DOI: 10.1103/PhysRevC.76.057001 PACS number(s): 21.30.−x, 24.70.+s, 25.10.+s, 13.75.Cs

A few nucleon systems are fundamental laboratories for the study of nuclear interactions. Among them, the system composed of three nucleons ($3N$) is the simplest nontrivial environment in which nucleon-nucleon (NN) force models can be tested. Though the $3N$ system properties at not-too-high energies are determined mainly by pairwise nucleon-nucleon interactions, additional dynamics related to the presence of the third nucleon, the so-called three nucleon force (3NF), is clearly needed. It is introduced to the theoretical formalism by means of semiphenomenological models such as the Tucson-Melbourne (TM) 3NF [1]. Its basic ingredient is the excitation of one of the nucleons into an intermediate Δ via a 2π exchange with the other two nucleons. Alternatively, 3NF can be generated by an explicit treatment of the Δ isobar excitation [2]. When the chiral perturbation theory (ChPT) is used at the next-to-next-to-leading order (NNLO), the $3N$ contributions arise naturally, fully consistently with the NN force terms [3]. Rich experimental evidence of the importance of the additional dynamics in $3N$ systems stems at present from the nucleon-deuteron elastic scattering observables. The picture emerging from comparisons of various data with theoretical predictions is, however, not fully consistent. In several cases, where the NN forces alone fail to reproduce the observables, the inclusion of 3NF leads to significant improvements [4–12] (for earlier references, see Ref. [13]). There are also cases when discrepancies between the experimental data and theoretical predictions remain if the presently available $3N$ dynamics is employed. For some cases, especially for various polarization observables [6–8,12,14], the NN+3NF calculations lead to a worse description of the data than the ones using just pure NN forces. This may indicate that some ingredients are still missing in the assumed dynamics, in particular in the spin-dependent part of the present models of 3NF.

For further tests and developments of the 3NF models, a large basis of precise data is necessary, while even in the case of the elastic scattering process there are still regions of energies and observables for which the information is not abundant. It is the case for deuteron polarization observables in the energy domain between 50 and 200 MeV per nucleon, where significant 3NF effects are predicted, while Coulomb and relativistic effects are practically negligible [15–17]. A systematic study at deuteron beam energies between 75 and 190 MeV [18] provided tensor and vector analyzing powers, but their precision is not sufficient to allow a quantitative comparison of descriptions given by various models. Later developments of ion sources and experimental techniques provided tools to achieve the required precision, but up to now only a few measurements have been performed. Most of them were carried out at RIKEN facility: deuteron vector and tensor analyzing powers were measured over almost the whole angular range at deuteron beam energies of 140, 200, and 270 MeV [9,12,19], and at 130 MeV these observables were studied with the setup covering about 50° range in the center-of-mass frame [20]. Moreover, deuteron-to-proton polarization transfer coefficients were measured at 270 MeV [12]. At the IUCF, a set of polarization observables—deuteron analyzing powers and spin correlation coefficients—was measured for pd elastic scattering with a polarized deuteron target [21]. These studies

*Present address: elzbieta.stephan@us.edu.pl
†Present address: Department of Physics, University of Teheran, Iran.
‡Present address: University of Winnipeg, Canada.

were performed at the high energy end of the energy domain considered here, with proton beam energies of 135 and 200 MeV.

The deuteron analyzing power data presented in this paper were measured with the 130 MeV deuteron beam at Kernfysisch Versneller Instituut (KVI), Groningen. The angular range of this measurement, covering over 100° in the center-of-mass frame, partially overlaps the previously measured data at this energy [20], which allows the determination of the beam polarization, as described below. The experiment was optimized for studies of the breakup process in a large phase space region, for which large acceptance, high statistics of the data and good angular resolution were required. Fulfilling these demands was also very advantageous for acquiring high precision elastic scattering data. Here we only briefly describe the experimental arrangement and data analysis procedure, more details are given in Refs. [22,23].

Polarized deuterons were produced in the KVI atomic beam polarized ion source (POLIS) [24] in seven states corresponding to various combinations of vector and tensor polarizations (P_Z, P_{ZZ}): (0, 0), (2/3, 0), (−2/3, 0), (0, 1), (0, −2), (1/3, 1), (1/3, −1). The values in brackets denote maximal theoretical values for 100% efficient transitions between the states of atomic deuterium. To minimize the contribution of accidental coincidences, the measurement was carried out with a very low beam current of about 40 pA, precisely measured in the Faraday cup. The vector and tensor polarized deuteron beam, accelerated in AGOR cyclotron to 130 MeV, was focused to a spot approximately 2 mm in diameter on a 6 mm thick liquid hydrogen target. The experimental setup, small angle large acceptance detector (SALAD), consisted of a three-plane multiwire proportional chamber (MWPC) and two layers of a segmented scintillator hodoscope: transmission ΔE and stopping E detectors. Position information from the MWPC was used for reconstruction of the particle emission angles, while the hodoscope allowed us to identify the particles, determine their energies, and define trigger conditions. The detection system covered the range between about 10° and 35° in the polar angles θ and the full (2π) range of the azimuthal angles φ. Data readout and acquisition systems were optimized for high throughput. Digitizing modules (analog-to-digital and time-to-digital converters) in the Fast Encoding and Readout Arrangement (FERA) standard were used, and a proportional chamber operating system (PCOS) readout was integrated at the end of the FERA chain. All the data were sent to two VME memories, working in the alternative buffering mode. The acquisition was controlled with the use of the GSI data acquisition system, Multi Branch System (MBS) [25] by the front-end processor RIO2, operating under a LynxOS real-time system. Dead time of the readout and acquisition systems was monitored continuously and registered as scaler rates, acquired every second.

In the first step of the data analysis, elastic scattering events were selected. Protons were cleanly discriminated from deuterons on the basis of $\Delta E - E$ dependence. Within the acceptance of the SALAD detector, one can distinguish three classes of the elastic scattering events: (i) proton-deuteron coincidences when both particles are fully identified, (ii) proton-deuteron coincidences when deuterons have energies too low to reach the stopping detector, i.e., to be identified, and (iii) single deuterons. In the second category, a small (below 5%) admixture of breakup events is possible, which barely affects the results. Measurement of the time of the particle registration with respect to the rf signal allowed us to determine and subtract the contribution of accidental coincidences, which was below 1%. The well-reproduced correlation between the proton and deuteron emission angles confirms that there was, at a level below 0.3°, no systematic shift of the reconstructed polar angles. The high quality of the data is confirmed by the well-reproduced shape of the elastic scattering cross section distribution [23].

To study polarization observables, the elastic scattering events collected for each of the polarization states $P = (P_Z, P_{ZZ})$ were analyzed. Considering angular resolution of the detector, bins of 1° in the polar angle were chosen. The binning was applied to proton angles ($\theta_p^{\rm lab}$) or deuteron angles ($\theta_d^{\rm lab}$) for coincidence and single deuteron events, respectively. Laboratory polar angles close to 30° for single deuterons were rejected from the analysis, since $\Delta\theta_d^{\rm lab}$ of 1° in this region corresponds to few degrees in the center-of-mass system, resulting in large variations of the observables within the bin. For each polar angle, events were sorted with respect to the angle φ between the polarization direction and the scattering plane, with the binning of 10°. The obtained numbers of events have been normalized to the charge collected in the Faraday cup and corrected for dead time losses. After normalization, the numbers of the elastically scattered events $N_P^\theta(\varphi)$ for the selected polarization state P and polar angle θ were obtained as a function of the angle φ. On their basis, the ratio

$$f_P^\theta(\varphi) = \frac{N_P^\theta(\varphi) - N_0^\theta(\varphi)}{N_0^\theta(\varphi)} \tag{1}$$

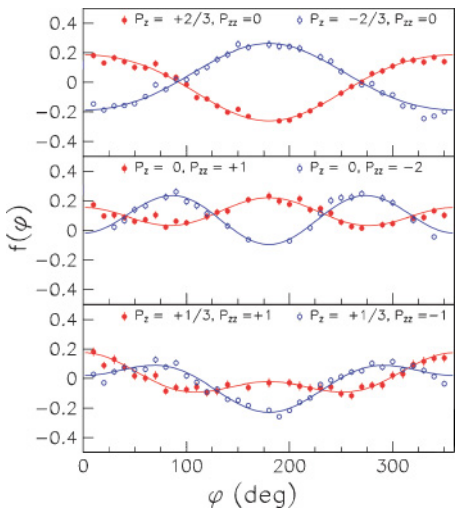

FIG. 1. (Color online) Ratios $f_P^\theta(\varphi)$ for six different polarization states for one chosen polar angle $\theta_d^{\rm c.m.} = 128.7°$ (symbols). The error bars represent statistical uncertainties. The nominal (maximal) polarization values are indicated in the panels. The lines are the results of the fit, as described in the text.

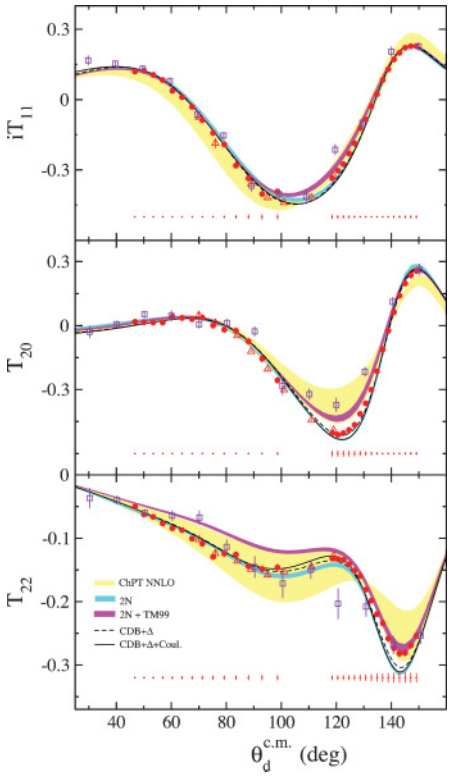

FIG. 2. (Color online) Vector and tensor analyzing powers for dp elastic scattering at 130 MeV: this work (dots), data from Ref. [18] (squares), and RIKEN data [20] (triangles). Theoretical predictions of different approaches are shown as lines and bands, as specified by the legend in the panel.

was constructed. $N_0^\theta(\varphi)$ denotes the analogously obtained number of events for the unpolarized beam. All factors constant in time, e.g., target thickness or detection efficiency, cancel in the ratio and thus do not have to be included in the normalization procedure.

Since the evaluated numbers of events are directly proportional to the corresponding cross sections, the formula for N_P^θ can be expressed by

$$N_P^\theta(\varphi) = N_0^\theta(\varphi)\cdot\Big[1 + iT_{11}(\theta)\sqrt{3}P_Z\cos\varphi - T_{22}(\theta)\frac{\sqrt{3}}{2}P_{ZZ}\cos 2\varphi - T_{20}(\theta)\frac{\sqrt{2}}{4}P_{ZZ}\Big], \quad (2)$$

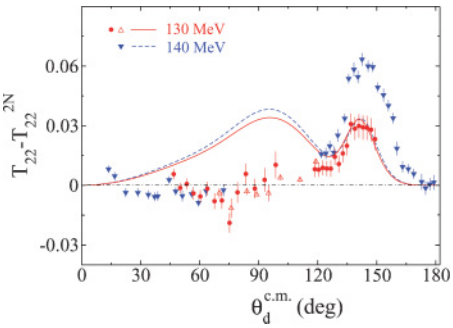

FIG. 3. (Color online) Net effect of 3NF for the T_{22} data measured at beam energies of 130 MeV (full dots, this work; open triangles, Ref. [20]) and 140 MeV (full triangles, Ref. [12]).

where $iT_{11}(\theta)$ and $T_{22}(\theta)$, $T_{20}(\theta)$ are spherical vector and tensor analyzing powers, respectively. Substituting formula (2) into Eq. (1) results in the final expression for the ratio $f_P^\theta(\varphi)$ as a function of the angle φ:

$$f_P^\theta(\varphi) = iT_{11}(\theta)\sqrt{3}P_Z\cos\varphi - T_{22}(\theta)\frac{\sqrt{3}}{2}P_{ZZ}\cos 2\varphi - T_{20}(\theta)\frac{\sqrt{2}}{4}P_{ZZ}. \quad (3)$$

Fit of the function given in Eq. (3) to the experimental $f_P^\theta(\varphi)$ distribution can be used to obtain polarization values if the analyzing powers are known; or vice versa, with the known polarization values, one is able to extract analyzing powers. In the region of $\theta_d^{\text{c.m.}} \leqslant 119^\circ$, values of the analyzing powers were determined in a separate, dedicated experiment at RIKEN [20], using the absolute calibration of the beam polarization via the $^{12}C(\vec{d},\alpha)^{10}B*[2^+]$ reaction [26]. In our measurement, $\theta_d^{\text{c.m.}} = 119^\circ$ lies close to the low limit of the angular range in which dp coincidences were registered. Kinematical cuts set on coincidences ensure particularly clean selection of the elastic scattering events; therefore, at this angle we used the procedure outlined above to extract P_Z and P_{ZZ}. The results obtained for various polarization states are given in Table I. Systematic errors follow from systematic uncertainties of the analyzing powers used in the fit. The other approach is to use the whole set of points from the RIKEN experiment and to find the polarization values giving the best match of the analyzing power data from both measurements. This procedure leads to about 6% lower values of P_Z and P_{ZZ}. The difference reflects a slight difference in shapes of the analyzing power distributions

TABLE I. Beam polarization values obtained for various (P_Z, P_{ZZ}) states; for more details, see text.

(P_Z, P_{ZZ})	P_Z	ΔP_Z^{stat}	ΔP_Z^{sys}	P_{ZZ}	$\Delta P_{ZZ}^{\text{stat}}$	$\Delta P_{ZZ}^{\text{sys}}$
$(+\frac{1}{3}, -1)$	0.265	0.007	0.007	−0.731	0.041	0.019
$(+\frac{2}{3}, 0)$	0.450	0.009	0.010	−0.083	0.050	0.023
$(-\frac{2}{3}, 0)$	−0.469	0.009	0.010	0.063	0.052	0.002
$(0, +1)$	−0.058	0.006	0.002	0.517	0.053	0.016
$(0, -2)$	0.009	0.005	0.001	−1.372	0.031	0.032
$(+\frac{1}{3}, +1)$	0.219	0.011	0.006	0.611	0.091	0.020

obtained in these two measurements and follows from their overall systematic errors. Finally, we calculated averages of P_Z and P_{ZZ} following from these two approaches and assigned them a systematic error of $\pm 3\%$. The obtained values of P_Z and P_{ZZ} were subsequently used in fits for determination of the analyzing powers at all analyzed $\theta_d^{\text{c.m.}}$ angles. Examples of distributions for $\theta_d^{\text{c.m.}} = 128.7^\circ$ (corresponding to $\theta_d^{\text{lab}} = 25^\circ$) together with the fitted curves $f_P^\theta(\varphi)$ are shown in Fig. 1.

Good agreement of the analyzing power results obtained from different polarization states allows us to calculate their weighted average. The final results are compared in Fig. 2 with theoretical predictions obtained in various approaches and with the data points from the RIKEN experiment at 130 MeV [20] and from an older measurement at 131 MeV [18]. Our data are presented with the statistical uncertainties only. The main contribution to the systematic errors (shown separately at the bottom of each panel) propagates from the errors of polarizations and affects mainly the overall normalization factor.

In the case of vector analyzing power iT_{11}, all the models provide similar predictions, generally confirmed by the data. Above 90°, the calculations that included TM99 3NF (2N+TM99) differ slightly from the predictions with pure NN potentials (2N) and coupled-channel calculations (CDB+Δ), but the data do not favor any of them. The best description of T_{20} is given by calculations within the coupled-channel framework with the CD Bonn+Δ potential, while the predictions of the ChPT and 2N+TM99 calculations are in disagreement with the data. The most interesting is T_{22}, for which the largest effects of 3NF are predicted. For $\theta_d^{\text{c.m.}}$ below 120°, the conclusions reached in Ref. [20] are confirmed: pure 2N and CDB+Δ calculations are consistent with the data. However, at larger $\theta_d^{\text{c.m.}}$ the data points follow the 2N+TM99 predictions. ChPT calculations for T_{22} agree with the data over the whole angular range, but the theoretical uncertainty band is wide. For all studied observables, the effects of including Coulomb force into coupled-channel calculations (CDB+Δ+Coul.) are negligible (cf. Fig. 2).

To examine the behavior of T_{22} in more detail and to compare the results with the data measured at 140 MeV [12], the net effect of 3NF is studied in Fig. 3. We limit our discussion to predictions obtained with the CD Bonn potential. The T_{22} values obtained with the pure NN CD Bonn potential (T_{22}^{2N}) were subtracted from both the data points and the predictions obtained with inclusion of the TM99 3NF (T_{22}^{3N+2N}). The same procedure was applied for both beam energies.

Below 120°, most of the data points are consistent with zero, i.e., they are well described by the pure NN force predictions. At larger angles, the addition of the TM99 3NF improves the description significantly; but for the beam energy of 140 MeV, the predicted effect of 3NF is not large enough to reproduce the data.

The high precision of the analyzing power data allows us to test the theoretical predictions at a new level of accuracy. The results presented here support the conclusion, following also from earlier studies, that in this energy region various calculations provide quite a good description of data, but none of them reproduce all the details of the experimental distributions. This strongly indicates that more refined models of 3NF are needed.

We would like to express our gratitude to the AGOR accelerator group for developing the excellent beam and to Rob Kremers for his work on the POLIS source. Part of the numerical calculations was performed on the IBM Regatta p690+ of the NIC in Jülich, Germany.

[1] S. A. Coon and H. K. Han, Few-Body Syst. **30**, 131 (2001).
[2] A. Deltuva, R. Machleidt, and P. U. Sauer, Phys. Rev. C **68**, 024005 (2003).
[3] E. Epelbaum *et al.*, Phys. Rev. C **66**, 064001 (2002).
[4] H. Witala, W. Glockle, D. Huber, J. Golak, and H. Kamada, Phys. Rev. Lett. **81**, 1183 (1998).
[5] S. Nemoto, K. Chmielewski, S. Oryu, and P. U. Sauer, Phys. Rev. C **58**, 2599 (1998).
[6] H. Sakai *et al.*, Phys. Rev. Lett. **84**, 5288 (2000).
[7] K. Ermisch *et al.*, Phys. Rev. Lett. **86**, 5862 (2001).
[8] K. Hatanaka *et al.*, Phys. Rev. C **66**, 044002 (2002).
[9] R. V. Cadman *et al.*, Phys. Rev. Lett. **86**, 967 (2001).
[10] K. Ermisch *et al.*, Phys. Rev. C **71**, 064004 (2005).
[11] P. Mermod *et al.*, Phys. Lett. **B597**, 243 (2004).
[12] K. Sekiguchi *et al.*, Phys. Rev. C **70**, 014001 (2004).
[13] W. Glöckle *et al.*, Phys. Rep. **274**, 107 (1996).
[14] H. R. Amir-Ahmadi *et al.*, Phys. Rev. C **75**, 041001(R) (2007).
[15] A. Kievsky, M. Viviani, and L. E. Marcucci, Phys. Rev. C **69**, 014002 (2004).
[16] A. Deltuva, A. C. Fonseca, and P. U. Sauer, Phys. Rev. C **71**, 054005 (2005).
[17] H. Witała, J. Golak, W. Glöckle, and H. Kamada, Phys. Rev. C **71**, 054001 (2005).
[18] H. Witała *et al.*, Few-Body Syst. **15**, 67 (1993).
[19] K. Sekiguchi *et al.*, Phys. Rev. C **65**, 034003 (2002).
[20] H. Mardanpour *et al.*, Eur. Phys. J. A **31**, 383 (2007).
[21] B. v. Przewoski *et al.*, Phys. Rev. C **74**, 064003 (2006).
[22] St. Kistryn *et al.*, Phys. Rev. C **68**, 054004 (2003).
[23] St. Kistryn *et al.*, Phys. Rev. C **72**, 044006 (2005).
[24] H. R. Kremers and A. G. Drentje, AIP Conf. Proc. **421**, 502 (1997).
[25] H. G. Essel and N. Kurz, IEEE Trans. Nucl. Sci. **NS-47**, 337 (2000).
[26] K. Suda *et al.*, Nucl. Instrum. Methods Phys. Res. A **572**, 745 (2007).